Pressure Effects on Carbon Monoxide Rebinding to the Isolated α and β Chains of Human Hemoglobin†

Masashi Unno, Koichiro Ishimori, and Isao Morishima*
Division of Molecular Engineering, Graduate School of Engineering, Kyoto University, Kyoto 606-01, Japan
Toshihiro Nakayama and Kumao Hamanoue
Department of Chemistry, Kyoto Institute of Technology, Kyoto 606, Japan
Received May 20, 1991; Revised Manuscript Received August 20, 1991

ABSTRACT: The effects of pressure on the recombination kinetics of carbon monoxide binding to the isolated α and β chains of human adult hemoglobin at pH 7, ~20 °C, were studied by the use of millisecond and nanosecond laser photolyses. The kinetic data were analyzed on the basis of a simple three-species model, which assumes two elementary reaction processes of bond formation and ligand migration steps. The activation volume for each elementary step was obtained from the pressure dependence of the rate constants. A pressure-dependent activation volume change from negative to positive values in the bimolecular carbon monoxide association reaction was observed for both of the isolated chains. This finding is attributed to a change of the rate-limiting step from the bond formation step to the ligand migration step. For both of the isolated chains, the activation volumes for ligand migration into and from the protein were estimated as +12–16 and +7–11 $cm^3\ mol^{-1}$, respectively. These positive activation volumes for the ligand migration process may be caused by conformational fluctuations of proteins, that is, the conformational changes from "closed" to "open" structure. In the iron–ligand bond formation process, the activation volumes are −15 to −22 $cm^3\ mol^{-1}$, which are almost identical to that for the model heme complexes [Taube, D. J., Projahn, H.-D., van Eldik, R., Magde, D., & Traylor, T. G. (1990) *J. Am. Chem. Soc. 112*, 6880–6886]. Accordingly, the surrounding protein contributions to the activation volumes for the bond formation process could be small. A slight difference in the activation volumes between the isolated chains was found for each elementary step. This is discussed in relation to characteristic features of the dynamic aspects of the isolated α and β chains.

The ligand binding dynamics for hemoproteins have been a subject of extensive studies in the last decade, since they serve as a typical model of protein dynamics. Transient absorption spectroscopic studies have been shown to be useful for delineating the mechanism of the ligand binding reaction. Binding of a ligand to a heme iron from a solvent phase was observed on a millisecond time scale (Brunori et al., 1966; Noble et al., 1969; Geraci et al., 1969; Philo et al., 1988). In the nanosecond region, geminate ligand binding in 50–100 ns was observed (Duddel et al., 1979, 1980; Alpert et al., 1979; Friedman & Lyons, 1980; Olson et al., 1987). This nanosecond rebinding is a process in which the photodissociated ligand rebinds to the heme iron without having diffused into the surrounding solvent. From these millisecond and nanosecond kinetic studies, a three-species model has been proposed (Campbell et al., 1984) in which there are two elementary steps for the bimolecular association reaction. The first step is an entry of the ligand into the heme pocket, followed by ligand binding to the heme iron.

In the present work, we have undertaken the study of the carbon monoxide (CO) rebinding kinetics for the isolated α and β chains of human hemoglobin under high hydrostatic pressure using laser photolysis. The application of high-pressure techniques to studies of the ligand binding kinetics of hemoproteins has contributed significantly to a better understanding of protein dynamics (Hasinoff, 1974; Caldin & Hasinoff, 1975; Adachi & Morishima, 1989; Projahn et al., 1990; Taube et al., 1990; Unno et al., 1990; Frauenfelder et al., 1990). Pressure-dependent kinetic studies provide information on the volume profile of the ligand binding process. The activation volume, the difference in the partial molar volume between the activated complex and reactants, is very easily visualized and is sensitive to the dynamics associated with the reaction process. Therefore, it is expected that the high-pressure kinetic study may provide us with fruitful information about the ligand binding dynamics.

Structural and kinetic differences between the α and β chains of human hemoglobin have been suggested by many investigators. From X-ray crystallographic studies of human oxyhemoglobin, Shaanan (1983) demonstrated that the distal pocket in the liganded β subunit is more widely opened than the liganded α subunit, which is sterically hindered by adjacent distal residues. It has been suggested that ligands can access to and exit from the β-heme iron more rapidly than to and from the α-heme group in the tetrameric intact hemoglobin, at least for the R-state conformation (Gibson et al., 1969; Olson & Gibson, 1971; Reisberg & Olson, 1980; Mathews et al., 1989). In the case of the isolated chains of hemoglobin, Olson et al. (1987) concluded that the protein structure of the β-heme pocket is flexible and can accommodate ligands more readily than that of the α chain. From these structural and kinetic studies of the α and β chains of hemoglobin, different pressure-dependent kinetics and a resulting different volume profile are expected. Accordingly, we have studied the effects of pressure on CO binding to the isolated α and β chains of human hemoglobin and have examined whether or not the volume profiles for the isolated α and β chains are different. In addition, we also discuss in some detail the pressure-dependent activation volume change which was observed for CO

† This work was supported in part by Grants 62840013 and 02780235 from the Ministry of Education, Science and Culture of Japan (to I.M. and K.I.).
* To whom correspondence should be addressed.

0006-2960/91/0430-10679$02.50/0

rebinding to intact hemoglobin (Unno et al., 1990).

Materials and Methods

Preparation of the Isolated α and β Chains of Hemoglobin. Hemolysate was prepared by a standard method from whole blood samples obtained from a local blood bank. The isolated α and β chains were prepared in a carbon monoxide form as described by Kilmartin et al. (Kilmartin & Rossi-Bernadi, 1971; Kilmartin et al., 1973) and Gerai et al. (1967). The isolated chains were stored in the carbonmonoxy form in liquid nitrogen prior to use. The purity of the isolated β chain was judged to be free of mercury by titration with *p*-(hydroxymercuri)benzoate. All of the experiments were performed in 50 mM Tris buffer at pH 7, which contains 0.1 M Cl^-.

The buffer solution has been shown to exhibit no pressure-dependent pH change in the pressure region examined here (Neuman et al., 1973). The protein concentration was varied from 20 to 40 μM (heme), and it was determined as a carbonmonoxy form, using a millimolar extinction coefficient of 13.4 mM^{-1} at 540 nm on a heme basis. In order to remove the dissolved oxygen in the solution, repeated evacuation with pure N_2 gas was carried out. A small amount of sodium dithionite was added to remove the trace of oxygen. The concentration of CO was calculated on the basis of the Henry's coefficient of 1.04 mM atm^{-1}.

Laser Photolysis Measurements under High Pressure. Millisecond and nanosecond laser photolysis experiments under high pressure were carried out as described previously (Unno et al., 1990). In the millisecond laser photolysis experiments, Rhodamine 6G (Kodak) in methanol was used to produce an excitation flash at 590 nm with a half-peak duration of 300 ns. The monitoring beam was generated by a Xe lamp. The high-pressure photolysis experiments took place by using a four-window high-presusre cell and its inner capsule (Hara & Morishima, 1988).

In the nanosecond laser photolysis experiments, the second harmonic (347.2 nm) of a Q-switch ruby laser with a half-peak duration of 20 ns was used (Ushida et al., 1989). The monitoring beam was generated by a pulsed Xe lamp, and the probe light was focused onto the entrance slit of a monochromator and detected by a photomultiplier (HTV R666). An Iwatu storage oscilloscope was used to digitize the resulting signal. The flash profile was deconvoluted to remove the response time of the recording system. The high-pressure apparatus was the same as for the millisecond experiments.

Evaluation of the Rate Constants and the Activation Volumes. CO rebinding to the isolated α chain in a millisecond region was analyzed by simple bimolecular association rate constants. The time courses of 436-nm absorption at all pressures were fitted to

$$\Delta A_t = \Delta A_0 \exp(-k_{app}t) \quad (1)$$

where ΔA_t is the absorbance change at any time t, ΔA_0 is the total change (absorbance at $t = 0$ minus absorbance at $t = \infty$), and k_{app} is the observed first-order rate constant. Because the CO rebinding to the isolated β chain is biphasic, the time courses for all the pressures were fitted to

$$\Delta A_t = \Delta A_f \exp(-k_f t) + \Delta A_s \exp(-k_s t) \quad (2)$$

where k_f and k_s are the observed fast and slow first-order rate constants, respectively, and ΔA_f and ΔA_s are the amplitudes of the exponential expressions for the fast and slow phase, respectively.

On a nanosecond time scale, the rebinding time courses were fitted to

$$\Delta A_t = \Delta A_\infty + \Delta A_g \exp(-k_g t) \quad (3)$$

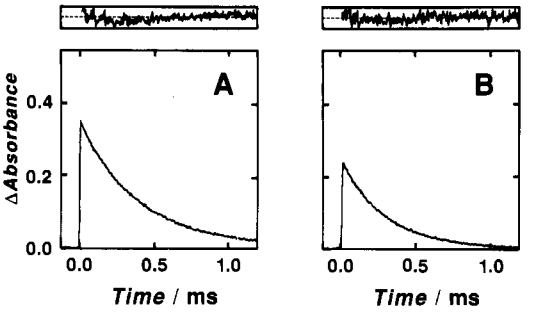

FIGURE 1: Millisecond time courses for the recombination of ~0.5 mM CO with the isolated α chains of human hemoglobin at two pressures: (A) 1 bar; (B) 1000 bar. The reactions were carried out at 20 °C and pH 7 in 50 mM Tris–0.1 M Cl^- buffer and were monitored at 436 nm. Protein concentrations were 22 μM (heme). 5-mm path-length cells were used. Photolysis was accomplished with a 300-ns laser flash (590 nm), and ~80% photolysis was obtained at atmospheric pressure. The upper side of the figure is the residuals from the best single-exponential fit (eq 1) to the time courses.

where ΔA_t and ΔA_∞ are the absorbance changes at time t and at the end of the geminate reaction, respectively, and k_g is the first-order geminate rate constant. ΔA_g is the extrapolated zero time absorbance change associated with geminate recombination. The fractional recombination yield, ϕ (geminate yield), can be calculated from the parameters in eq 3:

$$\phi = \frac{\Delta A_g}{\Delta A_\infty + \Delta A_g} \quad (4)$$

The rate constants for the elementary steps can be determined by

$$k_{21} = k_g\phi$$
$$k_{23} = k_g(1 - \phi) \quad (5)$$
$$k_{32} = k_{on}/\phi$$

where k_{21} is the bond formation rate, k_{23} is the rate for ligand escape, and k_{32} is the second-order rate constant for ligand migration to the geminate state.

The activation volume is given by

$$\Delta V^* = -RT\left(\frac{\partial \ln k}{\partial p}\right)_T \quad (6)$$

R is the gas constant (=8.314 J K^{-1} mol^{-1}), k is the rate constant, and 293.15 K was used for the value of T. The slope $(\partial \ln k/\partial p)_T$ for the α chain at atmospheric pressure was calculated from the optimized fourth-order polynomial function. Third-order functions were used for the function of the β chain. Curve fits were performed from 1 to 1500 bar for the α chain and from 1 to 900 bar for the β chain.

Results

Pressure Effects on the Apparent Quantum Yield and the Geminate Yield. Time courses for CO rebinding to the isolated α and β chains in the millisecond region at various pressures are shown in Figures 1 and 2. The most characteristic feature of Figures 1 and 2 is the decrease of the apparent quantum yield for the millisecond region at elevated pressures. The apparent quantum yield was reduced from 0.8 (1 bar) to ~0.5 (1000 bar) for both chains. This pressure-induced apparent quantum yield change was also observed for intact hemoglobin (Unno et al., 1990) and was attributed to an increase in the formation of the nanosecond geminate recombination (geminate yield). In an effort to confirm the increase of the geminate yield for the isolated α and β chains under high pressure,

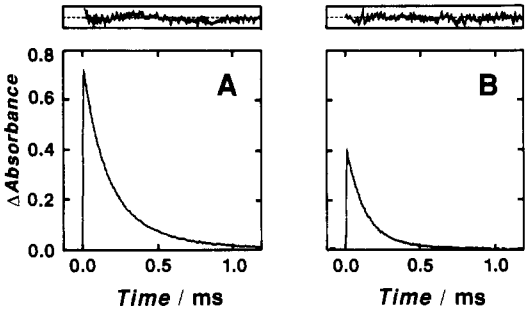

FIGURE 2: Millisecond time courses for the recombination of ~0.5 mM CO with the isolated β chains of human hemoglobin at two pressures: (A) 1 bar; (B) 1000 bar. Protein concentrations were 34 μM (heme). Experimental conditions are listed in Figure 1. The upper side of the figure is the residuals from the best two-exponential fit (eq 2) to the time courses.

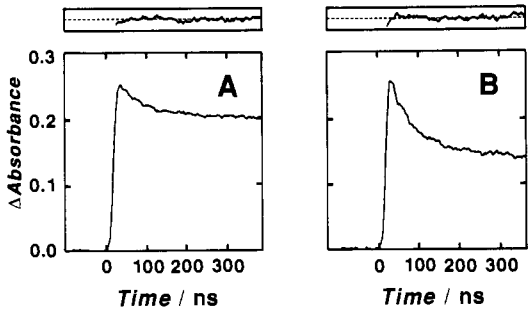

FIGURE 3: Nanosecond time courses for CO recombination with the isolated α chains of human hemoglobin at two pressures: (A) 1 bar; (B) 1000 bar. The reactions were carried out at room temperature (~20 °C) and pH 7 in 50 mM Tris–0.1 M Cl^- buffer and monitored at 436 nm. Protein concentrations were 36 μM (heme). 5-mm path-length cells were used, and the CO concentration was ~0.4 mM. Photolysis was accomplished with a 20-ns excitation-pulse (347.2 nm). The geminate yields were as follows: 1 bar, 0.2; 1000 bar, 0.5. The upper side of the figure is the residuals from the best exponential fit (eq 3) the the time courses.

we carried out nanosecond laser photolysis experiments under high pressure. Figures 3 and 4 show some typical recombination reactions under different pressures. It is readily noticed that the portion of the rebinding in the nanosecond region increases with pressurization. At atmospheric pressure, the geminate yield was about 0.2 and increased to about 0.5 at 1000 bar for both chains. It is also likely that pressure-induced spectral changes for deoxy- and carbonmonoxy isolated chains affect the absorbance changes for photodissociation. However, the difference in the absorbance at 436 nm was almost insensitive to pressure.[1] Therefore, the low apparent quantum yield at high pressure mainly arises from an increase in the geminate yield, as previously found for intact hemoglobin (Unno et al., 1990).

Pressure Effects on the Bimolecular Association Rate and Geminate Rate Constants. On a millisecond time scale, the binding of CO to the isolated α chain appears as a simple bimolecular association reaction. The upper side of Figure 1 depicts the residuals from the best exponential fit to the time courses. The residuals at 1000 bar exhibit a random distribution about a mean value of zero, indicating that the time courses can be fit to a single-exponential expression under high pressure. The bimolecular association rate constant at normal pressure amounts to $(5.08 \pm 0.03) \times 10^6$ M^{-1} s^{-1}, and this value is virtually identical to that reported previously (Antonini & Brunori, 1970; Reisberg & Olson, 1980; Mims et al., 1983). In contrast to the isolated α chain, photolysis of the carbonmonoxy β chain gives biphasic rebinding kinetics (Philo et al., 1988). This binding heterogeneity was also encountered under high pressure, and the kinetic data were fitted by eq 2. The upper side of Figure 2 shows the residuals from the best biexponential fit to the time courses, and two exponentials are required to fit the kinetic data without systematic deviations. The bimolecular association rate constants at normal pressure are $k_{fast} = (1.29 \pm 0.04) \times 10^7$ M^{-1} s^{-1} and $k_{slow} = (4.58 \pm 0.14) \times 10^6$ M^{-1} s^{-1}. These values are consistent with those reported by Philo et al. (1988). Under the experimental condition, the fast phase is a major component (~70%).

[1] M. Unno, K. Ishimori, and I. Morishima, unpublished results.

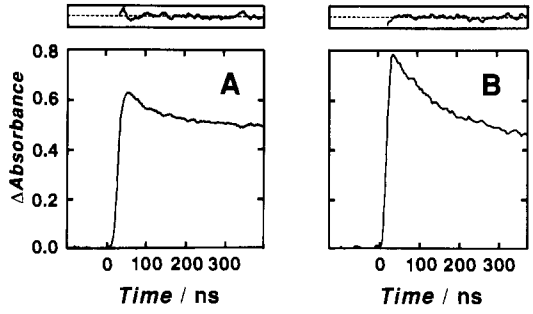

FIGURE 4: Nanosecond time courses for CO recombination with the isolated β chains of human hemoglobin at two pressures: (A) 1 bar; (B) 1000 bar. Protein concentrations were 39 μM (heme). The geminate yields were as follows: 1 bar, 0.2; 1000 bar, 0.5. Experimental conditions are listed in Figure 3. The upper side of the figure is the residuals from the best exponential fit (eq 3) to the time courses.

Table I: Typical Empirical Parameters for CO Bimolecular Association Recombination with the Isolated α and β Chains of Human Hemoglobin at Various Pressures[a]

P (bar)	α-chain k_{on} ($\times 10^{-6}$ M^{-1} s^{-1})	β-chain[b] k_{fast} ($\times 10^{-6}$ M^{-1} s^{-1})
1	5.08 ± 0.03	12.9 ± 0.4
500	6.40 ± 0.04	15.6 ± 0.6
1000	6.85 ± 0.08	15.9 ± 0.7
1500	6.16 ± 0.09	15.6 ± 0.6

[a] Typical data are shown in this table. Experiments were performed by the millisecond laser photolysis apparatus in 50 mM Tris–0.1 M Cl^-, pH 7 at 20 °C. The rate constants were obtained by fitting the observed absorbance traces to an exponential expresson (see text). The values listed represent the average of fits to three runs. Each run is an average of five to nine laser shots. The errors at atmospheric pressure are listed as the overall standard deviation from the mean, and the errors under high pressure were calculated using the propagation of error theory and the formula k_{on}(high pressure) = k_{on}(1 bar)k_p/k_1, where k_p and k_1 are observed first-order rate constants at high pressure and at normal pressure, respectively. [b] The values for the fast phase of the β chains are listed in this table.

Pressure caused substantial changes in the bimolecular association rates for both of the isolated chains. The bimolecular association rates at various pressures for the isolated α and the fast phase (major component) for the isolated β chain are listed in Table I, and $\Delta \ln k_{on}$ [=$\ln k_p$(at high pressure)/k_1(1 bar)] is plotted against pressure in Figure 5. The association rate for the isolated α chain was increased from $(5.08 \pm 0.03) \times 10^6$ (1 bar) to $(6.86 \pm 0.08) \times 10^6$ M^{-1} s^{-1} (1000 bar) and decreased to $(6.18 \pm 0.09) \times 10^6$ M^{-1} s^{-1} (1500 bar). Upon elevation of pressure from 1 to ~1100 bar, the association rate of the fast phase for the isolated β chain was increased from $(1.29 \pm 0.04) \times 10^7$ to $(1.64 \pm 0.08) \times 10^7$ M^{-1} s^{-1}, and it was decreased to $(1.56 \pm 0.06) \times 10^7$ M^{-1} s^{-1} in going from ~1100 to 1500 bar. High pressure also caused changes in the fraction of the fast and slow phases for the β chain. The spectral amplitude of the slow phase decreased with rising pressure, and the recombination reaction appears to consist of the fast phase only at 1500 bar (results not shown). Since the signal change for the slow phase is small

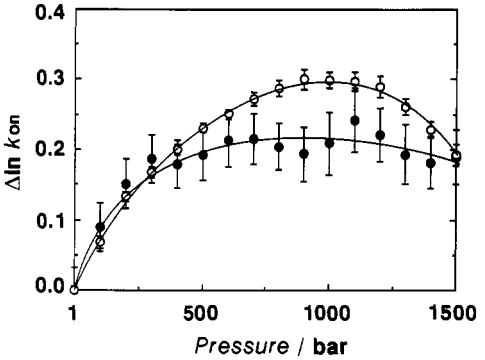

FIGURE 5: Logarithmic plots of the rate constants for the bimolecular CO association reaction versus pressure for the isolated α (○) and the fast phase of the isolated β (●) chains of human hemoglobin. Experiments were performed with a millisecond laser photolysis apparatus in 50 mM Tris–0.1 M Cl^-, pH 7, at 20 °C. The points were determined as described in the text, and the error bars were calculated using propagation of error theory (see Table I). The solid line was simply drawn through the points.

Table II: Typical Empirical Parameters for CO Geminate Recombination with the Isolated α and β Chains of Human Hemoglobin at Various Pressures[a]

	α chain		β chain	
P (bar)	k_g ($\times 10^6$ s^{-1})	ϕ	k_g ($\times 10^6$ s^{-1})	ϕ
1	15.8 ± 0.8	0.214 ± 0.012	9.25 ± 0.95	0.228 ± 0.022
500	16.0 ± 1.2	0.353 ± 0.023	8.72 ± 0.61	0.366 ± 0.015
1000	16.7 ± 0.6	0.507 ± 0.008	8.62 ± 0.40	0.474 ± 0.005
1500	21.6 ± 0.3	0.666 ● 0.005	9.26 ± 0.33	0.538 ± 0.005

[a] Typical data are shown in this table. Experiments were performed by a nanosecond laser photolysis apparatus in 50 mM Tris–0.1 M Cl^-, pH 7, at room temperature (~20 °C). The geminate rates, k_g, and the geminate yield, ϕ, were obtained by fitting the observed absorbance traces to an exponential expression (see text). The values listed represent the average of fits to 3 runs, each run being the average of 10 laser shots. The errors are listed as the standard deviation from the mean.

and the uncertainty in the parameters for the β chain is large, we could not successfully obtain the activation volumes for the slow phase of the β chain.

On a nanosecond time scale, the geminate rebinding of CO to the isolated α and β chains was characterized by a single exponential, and the rebinding time courses were fitted by eq 3. The upper sides of Figures 3 and 4 illustrate the residuals from the best fit to eq 3. We cannot rule out the possibility that the rebinding time courses are better fitted to a sum of two exponentials. However, the refinement is not pertinent to the central issues discussed below. Parameters at various pressures for both chains are collected in Table II. The geminate rate constants at normal pressure are 16×10^6 s^{-1} and 9×10^6 s^{-1} for the α and β chains, respectively, and are almost independent of pressure. The geminate yield for both chains is monotonously increased by pressure.

Pressure Effects on the Elementary Kinetic Steps. On the basis of the nanosecond laser photolysis experiments, the following simple scheme has been proposed to describe ligand binding to hemoproteins (Murray et al., 1988a,b):

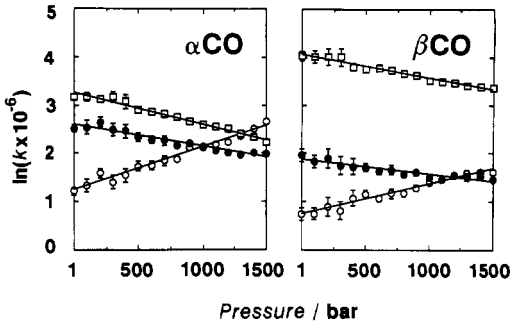

FIGURE 6: Logarithmic plots of the bond formation rate, k_{21} (○), the rate of ligand escape from the geminate state to the solvent, k_{23} (●), and the rate of ligand migration from the solvent to the geminate state, k_{32} (□), versus pressure. Experimental conditions are listed in Tables I and II. The straight lines are obtained by linear least-squares calculations. The determination of the points and error bars are listed in Table III.

$$\underset{1}{PCO} \underset{k_{12}}{\overset{k_{21}}{\rightleftharpoons}} \underset{2}{P{\cdot}CO} \underset{k_{23}}{\overset{k_{32}}{\rightleftharpoons}} \underset{3}{P + CO} \qquad (7)$$

PCO represents the bound state containing CO attached to the heme iron atom; P·CO, the geminate state formed after bond dissociation; and P + CO, a state where the CO molecule is in the solvent phase. Absorbance changes are only associated with the formation and decay of the PCO state. Assuming a steady-state population of the geminate state, the rate constants for the elementary steps of this kinetic scheme were obtained as described under Materials and Methods. The resulting elementary rate constants are listed in Table III. In order to obtain the activation volumes for each elementary step, these rate constants are plotted against pressure as the semilog plots in Figure 6. For both chains, the slopes of the linear plots for the ligand migration process (k_{23}, k_{32}) are positive, whereas that for the bond formation process (k_{21}) is negative. It is worth noting that pressurization reverses the relative magnitude of the bond formation rate (k_{21}) and ligand escape rate (k_{23}) at about 1000 bar for both chains. This implies that the ligand migration process is rate-determining under high pressure. The estimated activation volumes for the elementary steps at atmospheric pressure are collected in Table IV. Resulting volume profiles are schematically illustrated in Figure 7.

Discussion

Rate-Limiting Steps for the CO Binding Reaction under High Pressure. It has been reported that a negative activation volume is characteristic of the bond formation reaction of neutral molecules (le Noble, 1965), and yet the diffusion-controlled reaction of CO binding to protoheme in aqueous ethylene glycol and in glycerol experiences positive activation volumes (Caldin & Hasinoff, 1975). [The interpretation of

Table III: Typical Kinetic Parameters for a Three-Species Model of the Isolated α and β Chains of Human Hemoglobin under Various Pressures[a]

	α chain			β chain[b]		
P (bar)	k_{21} ($\times 10^6$ s^{-1})	k_{23} ($\times 10^6$ s^{-1})	k_{32} ($\times 10^6$ M^{-1} s^{-1})	k_{21} ($\times 10^6$ s^{-1})	k_{23} ($\times 10^6$ s^{-1})	k_{32} ($\times 10^6$ M^{-1} s^{-1})
1	3.37 ± 0.25	12.4 ± 0.9	23.7 ± 1.3	2.11 ± 0.30	7.14 ± 1.01	56.5 ± 5.8
500	5.66 ± 0.55	10.4 ± 1.0	18.1 ± 1.2	3.19 ± 0.26	5.53 ± 0.45	42.7 ± 2.3
1000	8.48 ± 0.31	8.24 ± 0.31	13.5 ± 0.3	4.09 ± 0.19	4.53 ± 0.22	33.5 ± 1.6
1500	14.4 ± 0.2	7.23 ± 0.11	9.24 ± 0.16	4.98 ± 0.18	4.28 ± 0.16	28.9 ± 1.2

[a] Typical data are shown in this table. The parameters were calculated from the empirical parameters (k_g, ϕ, k_{on}) by the three species model. The uncertainties were calculated using the propagation of the error theory and the formula $k_{21} = k_g\phi$, $k_{23} = k_g(1 - \phi)$, and $k_{32} = k_{on}/\phi$. [b] The values for the fast phase of the β chain are listed in this table.

Table IV: Volume of Activation (cm^3 mol^{-1}) for the Bimolecular Association Reaction and the Elementary Steps of CO Binding to the Isolated α and β chains of Human Hemoglobin[a]

protein	ΔV^*_{21}	ΔV^*_{23}	ΔV^*_{32}	ΔV^{*b}
α chain	−21.8 ± 0.9	11.1 ± 0.8	16.0 ± 0.6	−18.4 ± 0.5
β chain[c]	−15.4 ± 0.8	7.4 ± 0.7	12.1 ± 0.6	−22.4 ± 1.7

[a] Experimental conditions were 50 mM Tris–0.1 M Cl^-, pH 7, at 20 °C. The parameters were calculated from the slope, $(\partial \ln k/\partial p)_T$, of Figures 3 and 5 (see text). The errors are listed as the standard deviation from the mean. [b] The values for the bimolecular association reaction. [c] The values for the fast phase of β chains are listed in this table.

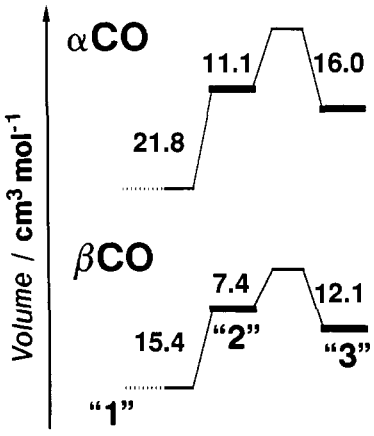

FIGURE 7: Volume profile for CO binding to the isolated α and β chains of human hemoglobin. The activation volumes for each elementary step are shown.

activation volumes has received wide attention and was reviewed extensively by Asano and le Noble (1978), van Eldik et al. (1989), and Frauenfelder et al. (1990).] The relationship between the activation volume and the rate-limiting steps was suggested by studies of pressure effects on ligand binding to myoglobin (Hasinoff, 1974; Adachi & Morishima, 1989; Projahn et al., 1990; Taube et al., 1990) and hemoglobin[2] (Hasinoff, 1974; Unno et al., 1990). The activation volumes of the bimolecular association reaction for the isolated α chain and those of the fast phase of the reaction for the isolated β chain of hemoglobin at atmospheric pressure are estimated here as −18.2 and −22.4 cm^3 mol^{-1}, respectively. Such negative activation volumes suggest that the iron–ligand bond formation process in the overall bimolecular association reaction predominates at ordinary pressure, which was previously suggested by Olson et al. (1987).

In contrast to the situation at atmospheric pressure, activation volumes at high pressure (>~1000 bar) for bimolecular association with the isolated α and β chains are positive (Figure 5). Since the ligand migration step is characterized by a positive activation volume, it is likely that the ligand migration process becomes rate-limiting at high pressure. However, measurements involving overall association cannot rule out the possibility that the pressure-induced activation volume change is caused by pressure-induced conformatioal changes. Since the nanosecond laser photolysis experiment offers information about the elementary steps, it provides clear evidence for a pressure-dependent alteration of the rate-limiting step. As shown in Figure 6 and Table III, the bond formation rate (k_{21}) is accelerated by pressure, and the ligand migration rates (k_{23}, k_{32}) are reduced for both isolated chains. The plots in Figure 6 are sufficiently linear for each elementary step, which suggests that pressure-induced conformational changes, if any, do not affect the elementary rate constants. Furthermore, k_{23} is larger than k_{21} at normal pressure, implying that the bond formation step is rate-determining. At about 1000 bar, however, k_{23} becomes greater than k_{21}, indicating that the ligand migration step becomes rate-determining under high pressure. On the basis of the present results, the free energy diagram for binding of CO to the isolated α and β chains of hemoglobin is shown schematically in Figure 8 (Murray et al., 1988a,b), where the free energy of the system is depicted as a function of the reaction coordinate. "1" represents the CO-bound state, "2" the geminate state, and "3" a state where CO is in the solvent phase. Under atmospheric pressure, the bond formation reaction at the heme iron is the rate-lmiting step and is represented as a solid curve in Figure 8. Taking into account that the bond formation rate (k_{21}) is accelerated and the ligand migration rate (k_{23}, k_{32}) is slowed down with increased pressure, the free energy profile under pressure may be depicted with the dushed curve, in accordance with the pressure-induced switching of the rate-limiting step from a bond formation to a migration process.

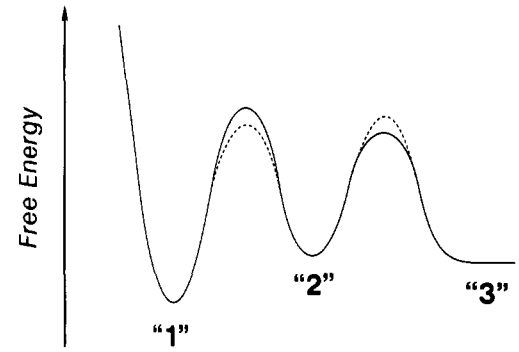

FIGURE 8: Relative free energy is plotted versus the reaction coordinate; "1" represents the CO-bound state; "2", the geminate state where CO is still in the heme pocket; "3", a state where CO is in the solvent phase. The solid curve is at atmospheric pressure, while the dashed curve is at high pressure.

Volume Profile for the CO Binding Reaction—Activation Volumes. Previous studies suggested that there are substantial differences in the ligand binding kinetics and heme environmental structures between the α and β subunits in the high-affinity form of intact hemoglobin (Gibson et al., 1969; Olson & Gibson, 1971; Reisberg & Olson, 1980; Shaanan, 1983; Mathews et al., 1989). The ligand binding site in the β subunits is less hindered and can easily accommodate a diatomic ligand molecule, judging from a comparison between the ligand assocation rate constants for native and mutant hemoglobin (Mathews et al., 1989) and from the crystallographic structure of oxyhemoglobin (Shaanan, 1983). Therefore, a marked difference in the activation volume profile between the isolated α and β chains is expected. However, Figure 7 clearly shows that both chains exhibit a similar activation volume profile: the volume first increases and then decreases to the value of the bound state. We now discuss in more detail the pressure effects on each of the two elementary steps: the ligand migration and the bond formation processes.

(A) Ligand Migration Process. For the ligand migration process through the protein to and from the heme pocket, the activation volumes are 16 and 11 cm^3 mol^{-1} for the isolated α chain, while those for the β chain are 12 and 7 cm^3 mol^{-1}, respectively. These positive activation volumes can be explained as follows. It was previously reported that the diffusion-controlled reaction such as CO binding to protoheme in

[2] In unpublished high-pressure kinetic work, M. Unno, K. Ishimori, and I. Morishima observed that millisecond O_2 rebinding to the intact and the isolated chains of hemoglobin whose rate-limiting step is considered to be a ligand migration process has a positive activation volume.

highly viscous solvents gives a positive activation volume (Caldin & Hasinoff, 1975). The CO migration rate constants (k_{32}) of the order of 10^7 M^{-1} s^{-1} for the isolated α and β chains under various pressures are roughly 10-fold less than the diffusion-controlled O_2 binding rate for the distally unhindered model heme compounds in unviscous solvents (Collman et al., 1983; Traylor et al., 1985). Therefore, the volume profiles in Figure 7 probably do not result from a simple ligand diffusion process, but from the dynamic conformational changes associated with the ligand migration process. Beece et al. (1980) suggested that proteins exist in a large number of conformational substates and can continuously move from one substate to another; motion of a ligand molecule inside a protein may be possible only through these conformational fluctuations. They proposed an "open and closed structure" model, which assumes that proteins have two conformational substates with "open" and "closed" structures. The ligand migration occurs readily for the open state but hardly at all for the closed state. On the basis of this model, the positive activation volume in the CO migration process could be associated with the protein conformational transition from the "closed" to the "open" state.

The positive activation volume in the ligand migration process was also observed for the reaction of ligand binding to myoglobin (Adachi & Morishima, 1989; Taube et al., 1990). Taube et al. (1990) also observed the positive activation volume for the ligand escape process and concluded that the positive activation volume may be attributed to conformational changes from the "closed" to "open" structure in myoglobin. Since the volume profile for the isolated chains exhibits similar features to that for myoglobin (Adachi & Morishima, 1989; Taube et al., 1990), such conformational changes from the "closed" to "open" structure in the CO migration process probably also describe the isolated α and β chains of hemoglobin.

(*B*) *Bond Formation Process.* From the available structural data of the R-state deoxy and CO hemoglobins, some explanations can be drawn for the negative activation volumes associated with the bond formation process. Because the Fe(II) atom is displaced $\sim$+0.3 and $\sim$−0.1 Å from the mean plane of the pyrrole nitrogens toward the proximal histidine (F8) for R-state deoxy and CO hemoglobins, respectively (Perutz et al., 1987; Derewenda et al., 1990), substantial changes in the protein conformation associated with this iron displacement could occur during carbonylation of hemoglobin. In addition, it has been suggested that the arrival of a ligand in the R-state hemoglobin leads to structural adjustments of the heme pocket so that the distal pocket valine residue (E11) moves to open a heme pocket (Luisi et al., 1990). However, the observed activation volume for the bond formation process (−15 to −22 cm^3 mol^{-1}) is almost identical to the activation volume (−19 cm^3 mol^{-1}) for the bimolecular addition of CO to the model heme complexes (Taube et al., 1990). Therefore, it appears quite reasonable that the iron–ligand bond-making process mainly contributes to the observed activation volumes. This implies that the other conformational factors such as motions of the surrounding protein do not contribute much to the activation volume in the bond formation process.

Comparisons between the Isolated α and β Chains. It has been suggested that the heme environmental structure in the high-affinity form of the α subunit is more constrained than the β subunit (Gibson et al., 1969; Olson & Gibson, 1971; Reisberg & Olson, 1980; Mathews et al., 1989), and this constraint is manifested as lower association rate constants for the α subunit, as shown in Table I. From the kinetic studies of alkyl isocyanide binding, Olson et al. (1987) showed that the geminate state in the isolated β chains is thermodynamically more stable than that for the isolated α chains. They interpreted these results as suggesting that the protein structure in the vicinity of the β-heme pocket is dynamically more flexible to readily accommodate these bulkier ligands, as compared with the α-heme pocket. This appears to be in accordance with the present finding that the activation volumes for the isolated β chains are a little bit smaller than those for the α chains.

The most puzzling aspect of the results for the isolated β chains is why pressure decreases the fraction of the slow rebinding phase. Results presented here agree with data reported by Philo et al. (1988), in that the time course of the bimolecular CO association reaction for the β chains is slightly biphasic. They also showed that the overall rebinding rate clearly increases with increasing protein concentration and proposed a concentration-dependent equilibrium between two conformers with CO association rates differing by a factor of 2.5. In the β_4 tetramer, the fast binding form is the main conformer, and the slow binding form is the minor one, whereas the β monomer lacks the fast binding form. Our present study has demonstrated that pressure increases the fraction of the fast phase, which would indicate that high pressure increases the fraction of the β_4 tetramer. However, it has frequently been found that high pressure facilitates dissociation of oligomeric proteins into their subunits (Penniston, 1971; Schade et al., 1980; Paladini & Weber, 1981; Fisher et al., 1986; Silva et al., 1989). It is thus likely that the tetramer–monomer equilibrium is not the entire story. There may be heterogeneity among monomer conformations, and high pressure may favor a monomeric form with fast CO binding properties for the isolated β chains.

In summary, high pressure decreases the apparent quantum yield for a millisecond recombination reaction of the isolated α and β chains of human hemoglobin, which is attributed to an increase in the fraction of the nanosecond geminate recombination reaction as found for the intact hemoglobin. The characteristic pressure dependence of the activation volume for the overall CO association reaction was characterized for both of the isolated chains. At atmospheric pressure, the activation volumes are negative, because the iron–ligand bond formation process dominates the rate-limiting step. At high pressure, however, the activation volume changed from negative to positive, due to switching of the rate-limiting step from bond formation to ligand migration.

It is quite interesting that both of the isolated chains exhibit similar activation volume profiles in the CO binding reaction (Figure 7), although many significant differences in the ligand binding kinetics and heme environmental structures between the isolated α and β chains of hemoglobin have been suggested. For both of the isolated chains, the activation volumes for the migration of ligand into the geminate state and for the escape of ligand from the protin to the solvent are all positive in sign. This is possibly attributed to a conformational fluctuation of the protein matrix. The activation volumes for the bond formation process for both of the isolated chains are negative and almost identical to those for the distally unhindered model heme compounds, implying that iron–ligand bond-making mainly contributes to the activation volume.

ACKNOWLEDGMENTS

We thank Dr. K. Ushida[3] (Kyoto Institute of Technology) for the nanosecond laser photolysis measurement and Dr. K.

[3] Present address: Institute of Physical and Chemical Research, Wako, Japan.

Hara (Kyoto University) and Dr. T. Takagi (Kyoto Institute of Technology) for the high-pressure experiment.

References

Adachi, S., & Morishima, I. (1989) *J. Biol. Chem. 264*, 18896–18901.

Alpert, B., El Mohsni, S., Lindqvist, L., & Tfibel, F. (1979) *Chem. Phys. Lett. 64*, 11–16.

Antonini, E., & Brunori, M. (1971) *Hemoglobin and Myoglobin in their Reaction With Ligands*, North-Holland Publishing Co., Amsterdam.

Asano, T., & le Noble, W. J. (1978) *Chem. Rev. 78*, 407–489.

Beece, D., Eisenstein, L., Frauenfelder, H., Good, D., Marden, M. C., Reinisch, L., Reynolds, A. H., Sorense, L. B., & Yue, K. T. (1980) *Biochemistry 19*, 5147–5157.

Brunori, M., Noble, R. W., Antonini, E., & Wyman, J. (1966) *J. Biol. Chem. 241*, 5238–5243.

Caldin, E. F., & Hasinoff, B. B. (1975) *J. Chem. Soc., Faraday Trans. 1 71*, 515–527.

Campbell, B. F., Magde, D., & Sharma, V. S. (1984) *J. Mol. Biol. 179*, 143–150.

Collman, J. P., Brauman, J. I., Iverson, B. L., Sessler, J. L., Morris, R. M., & Gibson, Q. H. (1983) *J. Am. Chem. Soc. 105*, 3052–3064.

Craescu, C. T., & Mispelter, J. (1988) *Eur. J. Biochem. 176*, 171–178.

Craescu, C. T., & Mispelter, J. (1989) *Eur. J. Biochem. 181*, 87–96.

Dalvit, C., & Wright, P. (1987) *J. Mol. Biol. 194*, 329–339.

Derewenda, Z. D., Dodson, G. G., Emsley, P., Harris, D., Nagai, K., & Perutz, M. F. (1990) *J. Mol. Biol.211*, 515–520.

Duddell, D. A., Morris, R. J., & Richards, J. T. (1979) *J. Chem. Soc., Chem. Commun.* 75–76.

Duddell, D. A., Morris, R. J., & Richards, J. T. (1980) *Biochim. Biophys. Acta 621*, 1–8.

Fisher, M. T., White, R. E., & Sligar, S. G. (1986) *J. Am. Chem. Soc. 108*, 6835–6837.

Frauenfelder, H., Alberding, N. A., Ansari, A., Braunstein, D., Cowen, B. R., Hong, M. K., Iben, I. E. T., Johnson, J. B., Luck, S., Maredn, M. C., Mourant, J. R., Ormos, P., Reinisch, L., Scholl, R., Schulte, A., Shyamusnder, E., Sorensen, L. B., Steinbach, P. J., Xie, A., Young, R. D., & Yue, K. T. (1990) *J. Phys. Chem. 94*, 1024–1037.

Friedman, J. M., & Lyons, K. B. (1980) *Nature (London) 284*, 570–572.

Gerai, G., Parkhurst, L. J., & Gibson, Q. H. (1969) *J. Biol. Chem. 244*, 4664–4667.

Gibson, Q. H., Parkhurst, L. J., & Geraci, G. (1969) *J. Biol. Chem. 244*, 4668–4676.

Hasinoff, B. B. (1974) *Biochemistry 13*, 4111–3117.

Kilmartin, J. V., & Rossi-Bernardi, L. (1971) *Biochem. J. 124*, 31–45.

Kilmartin, J. V., Fogg, J., Luzzana, M., & Rossi-Bernardi, L. (1973) *J. Biol. Chem. 248*, 7039–7043.

le Noble, W. J. (1965) *Prog. Phys. Org. Chem. 5*, 207–330.

Luisi, B., Bob, Liddington, B., Fermi, G., & Shibayama, N. (1990) *J. Mol. Biol. 214*, 7–14.

Mathews, A. J., Rohlfs, R. J., Olson, J. S., Tame, J., Renaud, J.-P., & Nagai, K. (1989) *J. Biol. Chem. 264*, 16573–16583.

Mims, M. P., Porras, A. G., Olson, J. S., Nobel, R. W., & Peterson, J. A. (1983) *J. Biol. Chem. 258*, 14219–14232.

Murray, L. P., Hofrichter, J., Henry, E. R., Ikeda-Saito, M., Kitagishi, K., Yonetani, T., & Eaton, W. A. (1988a) *Proc. Natl. Acad. Sci. U.S.A. 85*, 2151–2155.

Murray, L. P., Hofrichter, J., Henry, E. R., & Eaton, W. A. (1988b) *Biophys. Chem. 29*, 63–76.

Neuman, R. C., Jr., Kauzmann, W., & Zipp, A. (1973) *J. Phys. Chem. 77*, 2687–2691.

Noble, R. W., Gibson, Q. H., Brunori, M., Antonini, E., & Wyman, J. (1969) *J. Biol. Chem. 244*, 3905–3908.

Olson, J. S., & Gibson, Q. H. (1971) *J. Biol. Chem. 246*, 5241–5253.

Olson, J. S., Rohlfs, R. J., & Gibson, Q. H. (1987) *J. Biol. Chem. 262*, 12930–12938.

Paladini, A. A., & Weber, G. (1981) *Biochemistry 20*, 2587–2593.

Penniston, J. T. (1971) *Arch. Biochem. Biophys. 142*, 322–330.

Perutz, M. F., Fermi, G., Luisi, B., Shaanan, B., & Liddington, R. C. (1987) *Acc. Chem. Res. 20*, 309–321.

Philo, J. S., Lary, J. W., & Schuster, T. M. (1988) *J. Biol. Chem. 263*, 682–689.

Projahn, H.-D., Dreher, C., & van Eldik, R. (1990) *J. Am. Chem. Soc. 112*, 17–22.

Reisberg, P. I., & Olson, J. S. (1980) *J. Biol. Chem. 255*, 4151–4158.

Schad, B. C., Luedemann, H.-D., Rudolph, R., & Jaenicke, R. (1980) *Biochemistry 19*, 1121–1126.

Schaeffer, C., Craescu, C. T., Mispelter, J., Garel, M.-C., Rosa, J., & Lhoste, J.-M. (1988) *Eur. J. Biochem. 173*, 317–325.

Shaanan, B. (1983) *J. Mol. Biol. 171*, 31–39.

Silva, J. L., Villas-Boas, M., Bonafe, C. F. S., & Meirelles, N. C. (1989) *J. Biol. Chem. 264*, 15863–15868.

Taube, D. J., Projahn, H.-D., van Eldik, R., Magde, D., & Traylor, T. G. (1990) *J. Am. Chem. Soc. 112*, 6880–6886.

Traylor, T. G., Tsuchiya, S., Campbell, D., Mitchell, M., Stynes, D., & Koga, N. (1985) *J. Am. Chem. Soc. 107*, 604–614.

Unno, M., Ishimori, K., & Morishima, I. (1990) *Biochemistry 29*, 10199–10205.

Ushida, K., Nakayama, T., Hamanoue, K., Nagamura, T., Mugishima, A., & Sakimukai, S. (1989) *Rev. Sci. Instrum. 60*, 617–623.

van Eldik, R., Asano, T., & le Noble, W. J. (1989) *Chem. Rev. 89*, 549–688.